Letter

As-Li electrides under high pressure: Superconductivity, plastic, and superionic states

Zhongyu Wan [1], Wenjun Xu [1], Tianyi Yang [1], and Ruiqin Zhang [1,2,*]

[1] *Department of Physics, City University of Hong Kong, Hong Kong SAR 999077, People's Republic of China*

[2] *Beijing Computational Science Research Center, Beijing, 100193, People's Republic of China*

(Received 6 May 2022; revised 27 June 2022; accepted 1 August 2022; published 24 August 2022)

Inorganic electrides are a new class of compounds catering to the interest of scientists due to the multiple usages exhibited by interstitial electrons in the lattice. However, the influence of the shape and distribution of interstitial electrons on physical properties and new forms of physical states is still unknown. In this work, crystal structure search algorithms are employed to explore the possibility of forming unique electrides in the As-Li system, where interstitial electrons behave as one-dimensional (1D) electron chains (1D electride) in the *Pmmm* phase of $AsLi_7$ and transform into zero-dimensional (0D) electron clusters (0D electride) in the *P*6/*mmm* phase at 80 GPa. The *P*6/*mmm* phase has relatively high superconductivity at 150 GPa ($T_c = 38.4$ K) compared to classical electrides, even at moderate pressure with $T_c = 16.6$ K. In addition, a Dirac cone in the band has been observed, expanding the sources of Dirac materials. The survival of $AsLi_7$ at room temperature is confirmed by molecular dynamics simulation at 300 K. At 1000 K, the As atoms in the system act like a solid, while a portion of the Li atoms cycle around the As atoms, and another portion of the Li atoms flow freely like a liquid, showing the unusual physical phenomenon of the coexistence of the plastic and superionic states. This suggests that the superionic and plastic states cannot only be found in hydrides but also in the electride. Our results indicate that superconducting electride $AsLi_7$ with superionic and plastic states can exist in Earth's interior.

DOI: 10.1103/PhysRevB.106.L060506

Introduction. Inorganic electrides are a new class of compounds in which some of the surplus electrons in their crystal structure break away from the original atomic orbitals and enter into interstices [1], forming aggregated clusters in the interstices and acting as interstitial quasiatoms (ISQs) [2,3]. This has led to various novel properties and applications, in which the inorganic electrides act as catalytic [4], electrode [5], superconducting [6], and insulating materials [7]. In addition, modulating the distribution of interstitial electrons via changing chemical components or external conditions can lead to novel properties of the electride [8,9], such as the superconductivity by doping O atoms in the electride Nb_5Ir_3 [8], and the transformation of the insulating phase Ca_2N-II into the metallic Ca_2N-I by using high pressure [9]. This suggests that the shape of the ISQs also impacts their performance to a large extent [9,10]. Therefore, finding interstitial electrons with different shapes is key to expanding the application of electrides [11].

Unfortunately, their high electron activity makes most electrides extremely susceptible to decomposition under environmental conditions [12,13], resulting in the limited development of atmospheric pressure electrides. Recently, interstitial electrons induced under high-pressure conditions have been proved to form stable lattices, particularly in nonmetallic lithium-rich compounds such as Li-P [14,15], Li-C [16], and Li-Te [17] systems. This provides a new approach to the discovery of unknown electrides. At the same time, modulation of electronic structures by external pressure makes them promising as potential superconductors [18]. The element As has a similar electronegativity (2.20 vs 2.06, 2.50, and 2.01) and valence electron number compared to P, C, and Te [19], which suggests that unknown superconducting electrides maybe exist in the As-Li system. Therefore, in this work we perform a crystal structure search for lithium-rich compounds of arsenic at high pressures to find unique high-pressure electrides and physical properties with different shapes of interstitial electrons.

Computational Details. The CALYPSO software program [20] is used to perform a search for possible As_xLi_y ($x = 2$, $y = 2$–16) crystal structures at 50, 100, and 150 GPa. The Vienna *ab initio* simulation package (VASP) [21] is used to perform density functional calculations, with the projected augmented wave pseudopotentials method [22] to describe the electron-ion interaction, using $3d^{10}\,4s^2\,4p^3$ and $1s^2\,2s^1\,2p^0$ valence electronic structures of As and Li, respectively. Generalized gradient approximation of Perdew-Burke-Ernzerhof theory as exchange-correlated functional [23] are employed with a cutoff energy of 700 eV and k-point grid density of $0.03 \times 2\pi$ Å^{-1} based on the Monkhorst-Pack method [24]. The ionic positions and cell parameters are optimized with the criteria of energy and forces being 10^{-5}eV and 0.002 eV/Å, respectively. The ten lowest structures for each stoichiometric ratio are subjected to zero-point energy (ZPE) correction based on the quantum effects [25]. The PHONOPY [26] code was used to obtain the force constants of a $4 \times 4 \times 4$ supercell. Density functional perturbation theory [27] available in VASP is used to calculate the phonon dispersion curve. Based on the result of convergence tests (Table S1 in the Supplemental Material [28]), *ab initio* molecular dynamics (AIMD)

*aprqz@cityu.edu.hk

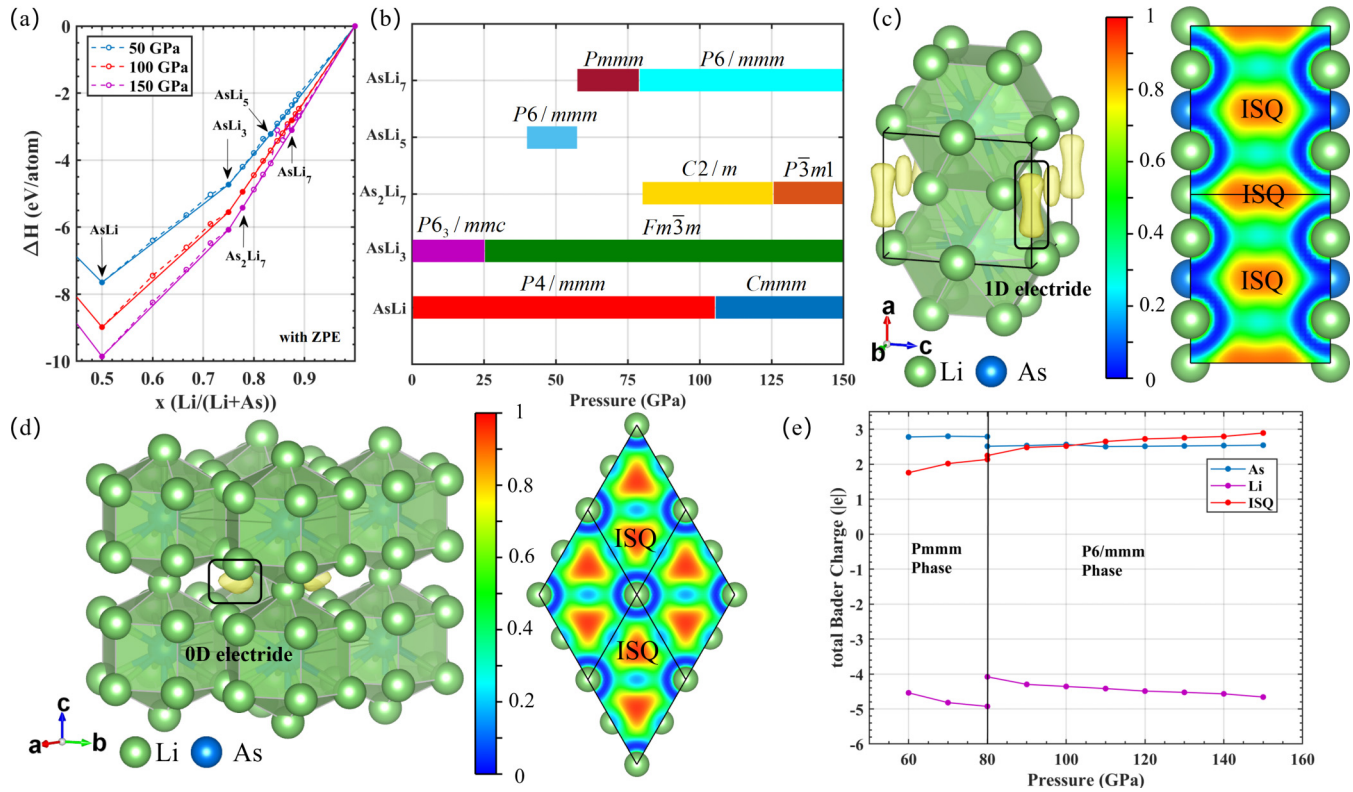

FIG. 1. (a) Convex hull of As-Li compounds at different pressures. (b) High-pressure phase diagram of stable As-Li compounds at 0–150 GPa. (c) ELF of *Pmmm* phase $AsLi_7$ at 80 GPa (isosurface = 0.85). (d) ELF of *P*6/*mmm* phase $AsLi_7$ at 150 GPa (isosurface = 0.85). (e) Bader charge of $AsLi_7$ from 60 to 150 GPa.

NVT simulations of a $3 \times 3 \times 2$ supercell containing only a Γ point with 144 atoms is performed for 7000 steps with a step size of 1 fs at the given temperature $T = 300$, 1000, and 2000 K with the Nosé-Hoover thermostat [29], respectively. The initial 2000 steps are used for thermalization and the remaining 5000 steps are used to calculate the statistical properties. The QUANTUM ESPRESSO package [30] is used to calculate the electron-phonon coupling (EPC) properties in linear response theory, using the ultrasoft pseudopotential with a cutoff energy of 120 Ry for As and Li. For *Pmmm* and *P*6/*mmm* based on $16 \times 12 \times 12$ and $16 \times 16 \times 12$ *k*-point grids, respectively, the Methfessel-Paxton first-order spread is set to 0.04 Ry, and their irreducible *q* points on the grids of $4 \times 3 \times 3$ and $4 \times 4 \times 3$ centered on Γ are used for first-order perturbation and dynamics matrix calculations. To investigate the effect of interstitial electrons on the electronic structure, fractional coordinates (0.4,0,0) and (0.6,0,0) of the *Pmmm* phase and fractional coordinates (0.67,0.33,0.5) and (0.33,0.67,0.5) of the *P*6/*mmm* phase are inserted by pseudoatoms with Wigner-Seitz radii of 1.2Å.

Results and Discussion. Convex-hull lines at 50, 100, and 150 GPa with 0 K are obtained by performing a crystal structure search [Fig. 1(a)]. Compounds located on the convex hull do not decompose into corresponding monomers [31,32] and other components are thermodynamically stable. In this system, ZPE has minimal effect on the thermodynamic properties (Table S2 in the Supplemental Material [28]). It can be seen that AsLi, $AsLi_3$, As_2Li_7, $AsLi_5$, and $AsLi_7$ are present on these lines, and their high-pressure phase diagrams from 0 to 150 GPa are derived by further refined structure searches [Fig. 1(b)]. The predicted atmospheric pressure structure [33] of $AsLi_3$ proves the credibility of the structure search. The electron localization function (ELF) is suggested [34] to be set to 0.85 to find electrides. However, only $AsLi_7$ exhibits strongly localized interstitial electrons in these compounds. It is stable as the *Pmmm* phase at 60 GPa and transforms to the *P*6/*mmm* phase at 80 until 150 GPa. Interestingly, the shapes of these interstitial electrons are entirely different. In the *Pmmm* phase [Fig. 1(c)], the As atom forms a supercoordinated 18-sided structural unit [$AsLi_{14}$] with 14 Li atoms, sharing a crystal plane between units, while the interstitial electrons are localized in a direction parallel to the *a* axis, forming a one-dimensional electron chain. In the *P*6/*mmm* phase, the supercoordinated structural unit [As-Li_{14}] remains constant, but only one crystal axis is shared between units, and the one-dimensional (1D) electron chain is transformed into a zero-dimensional (0D) electron cluster. Burton and co-workers [35] defined the dimension of electrides based on degrees of freedom of interstitial electrons; the interstitial electrons in 1D electrides exist in the shape of channels or chains, while the surplus electrons in 0D electrides are localized in a point or cluster. Based on this definition, the discovered $AsLi_7$ of *Pmmm* and *P*6/*mmm* are 1D and 0D electrides, respectively.

The phenomenon of supercoordination reveals anomalous charge transfer in the electride $AsLi_7$. To obtain the valence states of the different atoms, Bader charges [36] are employed for in-depth analysis [Fig. 1(e)]. As the pressure increases,

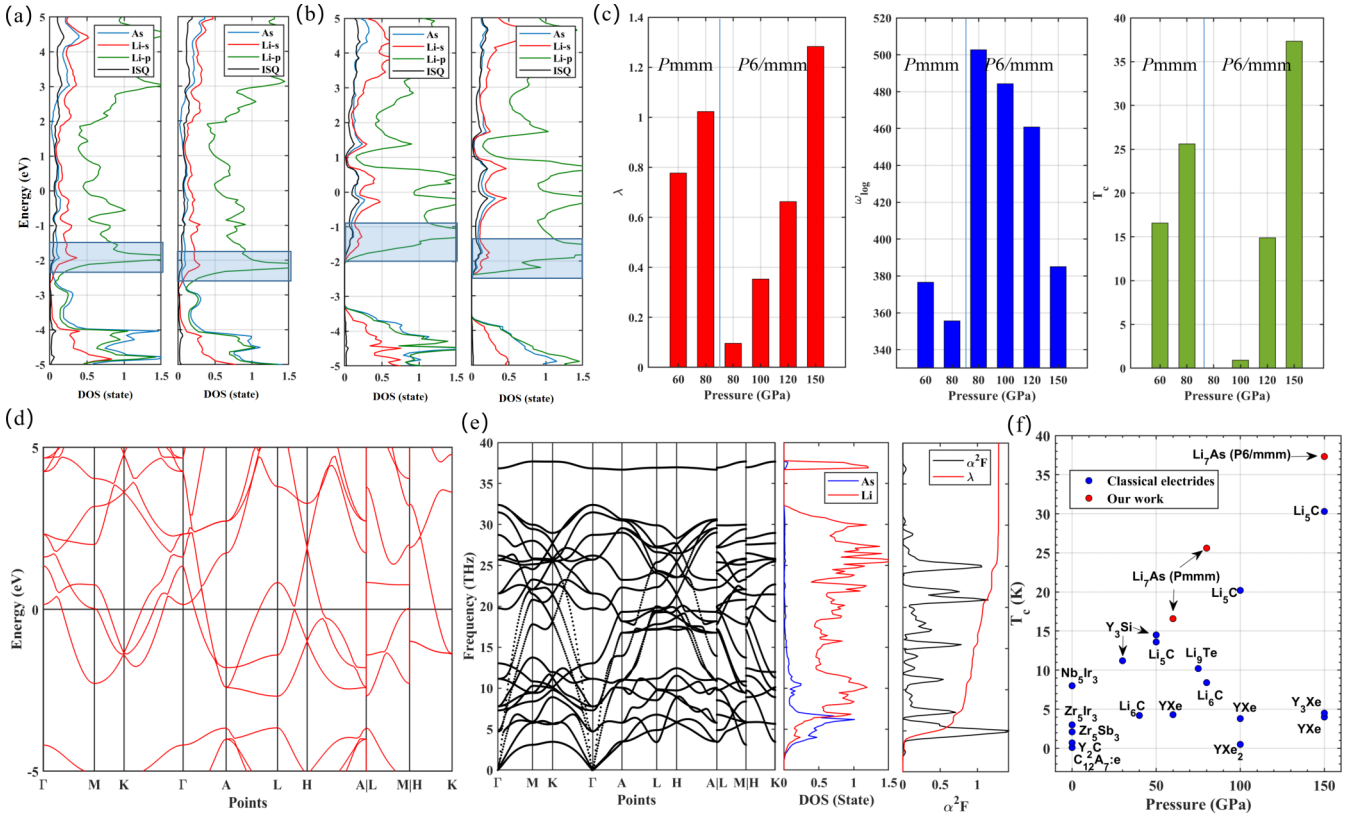

FIG. 2. (a) The density of states of *Pmmm* phase $AsLi_7$ at 60 and 80 GPa. (b) Density of states of *P*6/*mmm* phase $AsLi_7$ at 80 and 150 GPa. (c) Variation of EPC coefficients, $\omega_{\log}$, and T_c with pressure. (d) Electronic structure of the *P*6/*mmm* phase at 150 GPa. (e) Phonon dispersion curves, phonon density of states, and Eliashberg spectral functions for the *P*6/*mmm* phase at 150 GPa. (f) comparison of superconductivity with classical electrides [41,42].

the Bader charge of As remains constant for both the *Pmmm* and *P*6/*mmm* phases, while the Li atom and ISQ decrease and increase significantly, respectively, implying that Li atoms provide the interstitial electrons. This is because the 4*p* orbital of As is filled with three electrons and cannot accommodate any more electrons, while the pressure drives the interatomic distance shorter, leading to greater Coulomb repulsion and minimizing the energy of this system 2*s* electron of Li which breaks away from the nucleus into interstices. It is noteworthy that $AsLi_5$ does not exhibit obvious interstitial electrons. In the *P*6/*mmm* phase of $AsLi_5$, the distance between Li and its neighboring Li atoms ranges from 2.09 to 2.39 Å, which is higher than that of $AsLi_7$ in the *Pmmm* (from 2.00 to 2.25 Å) and *P*6/*mmm* phases (from 1.88 to 2.11 Å). Furthermore, the atomic densities of Li based on the cell volume are 0.097, 0.119, and 0.147 atoms/Å^3, respectively, indicating that the distribution of Li atoms in $AsLi_5$ is relatively sparse and the larger Li-Li distance prevents it from having interstitial electrons. Furthermore, we found a significant abrupt change in the total Bader charge of Li and As at the critical phase transition point of $AsLi_7$ at 80 GPa, because the average bond length of As-Li in the structural unit [$AsLi_{14}$] of the *Pmmm* phase is 2.224 Å. At the same pressure, the *P*6/*mmm* phase has 2.235 Å of As-Li in [$AsLi_{14}$]; the longer distance between As and Li makes the charge transport weaker, causing an abrupt decrease and increase of the Bader charges of As and Li at the phase transition point.

Given the effect of pressure on electron transfer, it is necessary to study its electronic structure modification and physical properties. From Figs. 2(a) and 2(b), it can be generalized that pressure can cause the overall density of electron states (DOS) to migrate downwards. It also explains the quasiatomic role of interstitial electrons, which are very close to As and Li-2*s*, although the DOS of ISQ at the Fermi level is not as much as Li-2*p*, suggesting a certain contribution of ISQ to the metallicity of electride $AsLi_7$. There are far more low-level DOS in As than high-level ones because the entire shell layer structure formed at the Fermi level prevents the As orbitals from reaching a higher level. In addition, As and Li atoms have similar trends at DOS, implying strong coupling between atoms and thus promising potential superconductors. It is noteworthy that *hP*4-Na exhibits a slight *d* character at high pressure, which suggests that higher *l*, *m* orbitals can be partially occupied by electrons in electrides. Our results (Fig. S4 [28]) show that the DOS of As *d* orbitals below the Fermi level is far less than that of *hP*4-Na in both the *Pmmm* and *P*6/*mmm* phase, suggesting that the As in $AsLi_7$ has no *d* character.

The modified McMillan-Allen-Dynes equation [37] calculates the superconducting properties at different pressures:

$$T_c = \frac{\omega_{\log}}{1.2k_B} \exp\left[-\frac{1.04(1+\lambda)}{\lambda - \mu^*(1+0.62\lambda)}\right], \qquad (1)$$

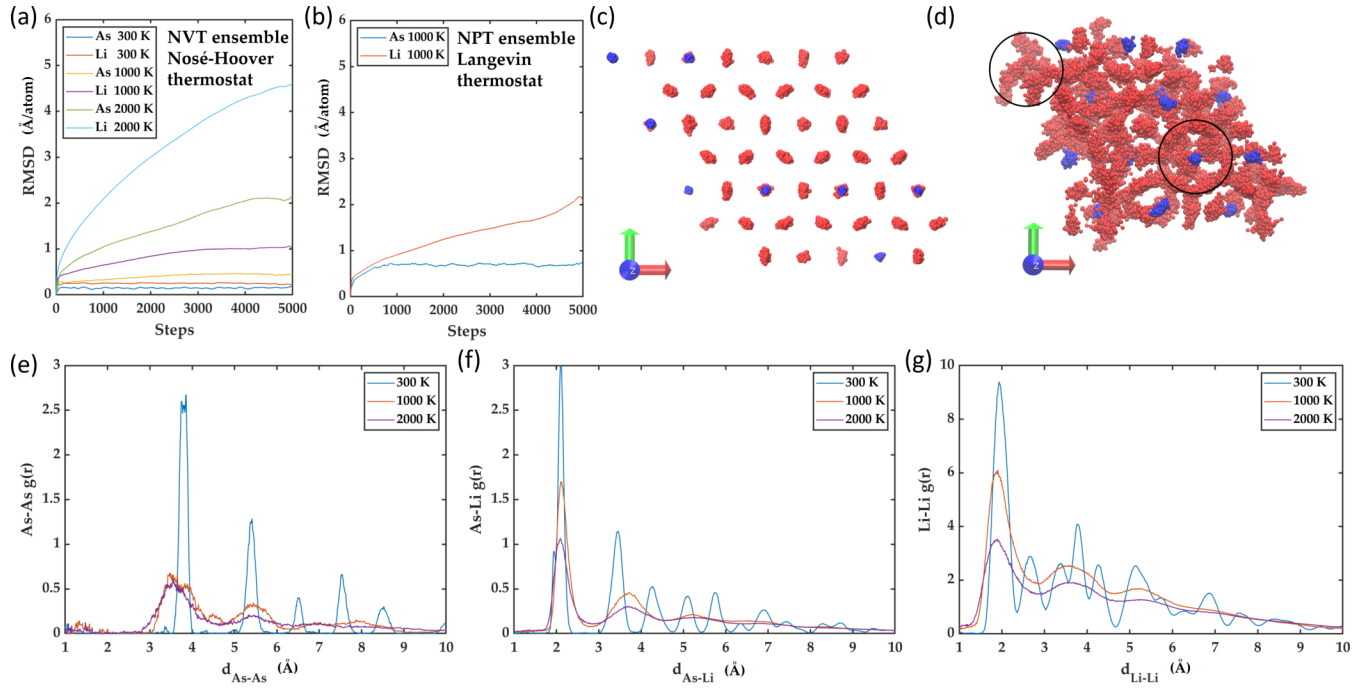

FIG. 3. (a) RMSD curves of As and Li at different temperatures with NVT condition. (b) RMSD curves of As and Li at 1000 K with NPT condition. (c) Trajectories at 300 K. (d) Trajectories at 1000 K. (e) RDF curves of As-As at different temperatures. (f) RDF curves of As-Li at different temperatures. (g) RDF curves of Li-Li at different temperatures.

where $\omega_{\log}$ is the log-averaged phonon frequency, k_B the Boltzmann constant, μ^* the Coulomb pseudopotential ($\mu^* = 0.10$), and λ the EPC constant. Figure 2(c) shows the variation of superconductivity with pressure, where the $P6/mmm$ phase has the highest λ, the smallest $\omega_{\log}$, and the largest T_c at 150 GPa. The physical properties are often determined by its electronic structures, and in order to obtain the physical insight and mechanism of the highest T_c, its band structure is shown in Fig. 2(d), which reveals that near the Fermi level, bands are flat in the $\Gamma \rightarrow M$ and $L \rightarrow M$ directions, in line with the "flat-steep band" characteristic [38] of general superconductors. We also find a Dirac cone [39] at the H point, suggesting that in addition to topological insulator surfaces [39] and Fe-based superconductors [40], it also exists in electrides with potentially high electron mobility and topological properties. Figure 2(e) shows the role of phonon dispersion on superconductivity. The absence of phonon spectra at imaginary frequencies indicates that it is kinetically stable, and the phonon DOS of the As atom is more concentrated at lower frequencies than in Li atoms due to its larger atomic mass. The calculated Eliashberg spectral function reflects a 66% contribution of phonons below 10 THz to the EPC constant at 150 GPa, implying that the superconductivity of the electride $AsLi_7$ is dominated by low-frequency phonons and that the strong electron-phonon coupling makes its superconductivity critical temperature higher than that of known electrides in the range of 0–150 GPa [41,42].

Our density functional theory (DFT) calculations are based on a temperature of 0 K, a condition far away from the actual environment, as can be seen by implementing AIMD at 300 K to obtain root mean square displacement curves (RMSD) for different atoms [Fig. 3(a)]. Whether it is As or Li, their RMSD remains constant, the slope of curves $k \approx 0$, indicating that there is no significant change in the displacement of the atoms, and the trajectories are shown in Fig. 3(c), where they act like solids, which means it can survive at room temperature. The temperatures of 1000 and 2000 K are further used to investigate the kinetic behavior of $AsLi_7$ at ultrahigh temperatures, and the RMSD curves at 1000 K show slopes $k_{As} \approx 0$ and $k_{Li} > 0$ for different atoms, indicating that the Li atoms are more liquidlike compared to As atoms which maintain a solid character. At temperatures up to 2000 K, there are results for $k_{As} > 0$ and $k_{Li} > 0$, proving that Li and As atoms behave as liquids and the whole system "melts." The atomic trajectories at 1000 K exhibit strange physical phenomena [Fig. 3(d)], with As atoms vibrating near their initial position, while some of the Li atoms move around the As (plastic state [43]) and some of the Li atoms flow freely (superionic state [44]). This shows that the plastic and superionic state can coexist in the electride $AsLi_7$ at this temperature. At 2000 K, all atoms become "liquid," confirming the "melting" of the system. The relationship between the "melting points" of different elements is concluded as $T_{Li} < T_{As}$. The energy homogeneity theorem and radial distribution functions (RDFs) of As-As, As-Li, and Li-Li [Figs. 3(e)–3(g)] also justify the simulation results, where the energy at equilibrium is evenly distributed between the degrees of freedom and the displacement of the atoms is stronger due to the lighter mass under the same kinetic energy conditions. Multiple peaks are clearly demonstrated in the RDF at 300 K. However, as the temperature increases, the height of the peaks decreases and they become broader, indicating a transition from the solid to the amorphous state. Besides, the NPT simulations based on the Langevin thermostat [45] get the same conclusion as

the NVT simulations based on the Nosé-Hoover thermostat [Fig. 3(b)], that is, $k_{As} \approx 0$ and $k_{Li} > 0$, which indicates that the superionic behavior at 1000 K indeed exists instead of a numerical artifact [46].

Since the Earth's interior [47] is also exposed to the same high-pressure and -temperature conditions and As and Li have high abundances within the Earth, we conjecture that the electron compound $AsLi_7$ can be found in it.

Conclusion. In this work, the possible phases of lithium-rich compounds of arsenic at high pressure are obtained by a structure search algorithm, and a series of high-pressure phase diagrams of As-Li are determined. $AsLi_7$ is found to be capable of forming 1D and 0D electrides in the phase of $Pmmm$ and $P6/mmm$, respectively. The Bader charge analysis confirms that the interstitial electrons are contributed by Li atoms. The $P6/mmm$ phase has the highest superconductivity at 150 GPa compared to classical electrides. In addition, the Dirac cone at the H point reveals potentially high electron mobility and topological properties, expanding the sources of Dirac materials. Further, AIMD confirms the possibility of existence at room temperature and the appearance of unusual coexistence of plastic and superionic states. Since the simulated environment of AIMD is close to that of the Earth's interior, so the electride may exist in it, providing a theoretical guide to the experimental discovery of unique matter.

Acknowledgements. The work described in this paper was supported by grants from the Research Grants Council of the Hong Kong SAR (Grants No. CityU 11305618 and No. 11306219) and the National Natural Science Foundation of China (Grant No. 11874081).

The authors declare that they have no known competing financial interests or personal relationships that could have appeared to influence the work reported in this paper.

[1] M. Miyakawa, S. W. Kim, M. Hirano, Y. Kohama, H. Kawaji, T. Atake, H. Ikegami, K. Kono, and H. Hosono, J. Am. Chem. Soc. **129**, 7270 (2007).
[2] X. Zhang, Z. Xiao, H. Lei, Y. Toda, S. Matsuishi, T. Kamiya, S. Ueda, and H. Hosono, Chem. Mater. **26**, 6638 (2014).
[3] M.-s. Miao and R. Hoffmann, J. Am. Chem. Soc. **137**, 3631 (2015).
[4] Y. Inoue, M. Kitano, S.-W. Kim, T. Yokoyama, M. Hara, and H. Hosono, ACS Catalysis **4**, 674 (2014).
[5] Z. Zhao, L. Liu, Y. Tong, G. Yang, and A. Bergara, J. Phys. Chem. C **121**, 21199 (2017).
[6] H. Hosono, S.-W. Kim, S. Matsuishi, S. Tanaka, A. Miyake, T. Kagayama, and K. Shimizu, Philos. Trans. R. Soc., A **373**, 20140450 (2015).
[7] Y.-M. Chen, H.-Y. Geng, X.-Z. Yan, Z.-W. Wang, X.-R. Chen, and Q. Wu, Chin. Phys. B **26**, 056102 (2017).
[8] Y. Zhang, B. Wang, Z. Xiao, Y. Lu, T. Kamiya, Y. Uwatoko, H. Kageyama, and H. Hosono, npj Quantum Mater. **2**, 45 (2017).
[9] Y. Zhang, W. Wu, Y. Wang, S. A. Yang, and Y. Ma, J. Am. Chem. Soc. **139**, 13798 (2017).
[10] Y. Tsuji, P. L. Dasari, S. Elatresh, R. Hoffmann, and N. Ashcroft, J. Am. Chem. Soc. **138**, 14108 (2016).
[11] Y. Zhang, Z. Xiao, T. Kamiya, and H. Hosono, J. Phys. Chem. Lett. **6**, 4966 (2015).
[12] J. L. Dye, Science **301**, 607 (2003).
[13] M. Kitano, Y. Inoue, Y. Yamazaki, F. Hayashi, S. Kanbara, S. Matsuishi, T. Yokoyama, S.-W. Kim, M. Hara, and H. Hosono, Nat. Chem. **4**, 934 (2012).
[14] Z. Zhao, S. Zhang, T. Yu, H. Xu, A. Bergara, and G. Yang, Phys. Rev. Lett. **122**, 097002 (2019).
[15] Z. S. Pereira, G. M. Faccin, and E. Z. da Silva, J. Phys. Chem. C **125**, 8899 (2021).
[16] Z. Liu, Q. Zhuang, F. Tian, D. Duan, H. Song, Z. Zhang, F. Li, H. Li, D. Li, and T. Cui, Phys. Rev. Lett. **127**, 157002 (2021).
[17] X. Zhang, F. Li, A. Bergara, and G. Yang, Phys. Rev. B **104**, 134505 (2021).
[18] J. Zhang, G. Chen, and H. Liu, J. Phys. Chem. Lett. **12**, 10388 (2021).
[19] A. L. Allred and E. G. Rochow, J. Inorg. Nucl. Chem. **5**, 264 (1958).
[20] Y. Wang, J. Lv, L. Zhu, and Y. Ma, Comput. Phys. Commun. **183**, 2063 (2012).
[21] G. Kresse and J. Furthmüller, Phys. Rev. B **54**, 11169 (1996).
[22] P. E. Blöchl, Phys. Rev. B **50**, 17953 (1994).
[23] J. P. Perdew, K. Burke, and M. Ernzerhof, Phys. Rev. Lett. **77**, 3865 (1996).
[24] J. D. Pack and H. J. Monkhorst, Phys. Rev. B **16**, 1748 (1977).
[25] T. H. Boyer, Ann. Phys. **56**, 474 (1970).
[26] A. Togo and I. Tanaka, Scr. Mater. **108**, 1 (2015).
[27] S. Baroni, S. De Gironcoli, A. Dal Corso, and P. Giannozzi, Rev. Mod. Phys. **73**, 515 (2001).
[28] See Supplemental Material at http://link.aps.org/supplemental/10.1103/PhysRevB.106.L060506 for electron localization functions of different As-Li compounds, crystal structure of $AsLi_7$, Li-Li lengths in $AsLi_5$ and $AsLi_7$, convergence test of molecular dynamics, ΔH and ΔU_{ZPE} of arsenic-lithium compounds, and electron density of states of As in $AsLi_7$.
[29] D. J. Evans and B. L. Holian, J. Chem. Phys. **83**, 4069 (1985).
[30] P. Giannozzi, S. Baroni, N. Bonini, M. Calandra, R. Car, C. Cavazzoni, D. Ceresoli, G. L. Chiarotti, M. Cococcioni, and I. Dabo, J. Phys.: Condens. Matter **21**, 395502 (2009).
[31] J. Lv, Y. Wang, L. Zhu, and Y. Ma, Phys. Rev. Lett. **106**, 015503 (2011).
[32] P. Tsuppayakorn-Aek, W. Luo, R. Ahuja, and T. Bovornratanaraks, Sci. Rep. **8**, 3026 (2018).
[33] M. Seel and R. Pandey, Int. J. Quantum Chem. **40**, 461 (1991).
[34] A. A. Dyachenko, A. V. Lukoyanov, V. I. Anisimov, and A. R. Oganov, Phys. Rev. B **105**, 085146 (2022).
[35] C. Liu, S. A. Nikolaev, W. Ren, and L. A. Burton, J. Mater. Chem. C **8**, 10551 (2020).
[36] M. Kosa and D. T. Major, CrystEngComm **17**, 295 (2015).
[37] K. Kitazawa, M. Naito, T. Itoh, and S. Tanaka, J. Phys. Soc. Jpn. **54**, 2682 (1985).
[38] F. J. Ribeiro, P. Tangney, S. G. Louie, and M. L. Cohen, Phys. Rev. B **74**, 172101 (2006).
[39] Y. Xia, D. Qian, D. Hsieh, L. Wray, A. Pal, H. Lin, A. Bansil, D. Grauer, Y. S. Hor, and R. J. Cava, Nat. Phys. **5**, 398 (2009).

[40] Y. Tanabe, K. Huynh, S. Heguri, G. Mu, T. Urata, J. Xu, R. Nouchi, N. Mitoma, and K. Tanigaki, Phys. Rev. B **84**, 100508(R) (2011).
[41] X. Zhang and G. Yang, J. Phys. Chem. Lett. **11**, 3841 (2020).
[42] H. Hosono and M. Kitano, Chem. Rev. **121**, 3121 (2021).
[43] H. Gao, C. Liu, A. Hermann, R. J. Needs, C. J. Pickard, H.-T. Wang, D. Xing, and J. Sun, Natl. Sci. Rev. **7**, 1540 (2020).
[44] C. Liu, H. Gao, A. Hermann, Y. Wang, M. Miao, C. J. Pickard, R. J. Needs, H.-T. Wang, D. Xing, and J. Sun, Phys. Rev. X **10**, 021007 (2020).
[45] B. Grabowski, L. Ismer, T. Hickel, and J. Neugebauer, Phys. Rev. B **79**, 134106 (2009).
[46] A. B. Belonoshko, J. Fu, and G. Smirnov, Phys. Rev. B **104**, 104103 (2021).
[47] C. Liu, H. Gao, Y. Wang, R. J. Needs, C. J. Pickard, J. Sun, H.-T. Wang, and D. Xing, Nat. Phys. **15**, 1065 (2019).